IOPscience iopscience.iop.org

Home Search Collections Journals About Contact us My IOPscience

Study on fatigue and breakdown properties of Pt/(Pb,Sr)TiO_3/Pt capacitors

This article has been downloaded from IOPscience. Please scroll down to see the full text article.

2006 J. Phys.: Condens. Matter 18 10457

(http://iopscience.iop.org/0953-8984/18/46/013)

View the table of contents for this issue, or go to the journal homepage for more

Download details:
IP Address: 129.252.86.83
The article was downloaded on 28/05/2010 at 14:30

Please note that terms and conditions apply.

INSTITUTE OF PHYSICS PUBLISHING JOURNAL OF PHYSICS: CONDENSED MATTER

J. Phys.: Condens. Matter **18** (2006) 10457–10467 doi:10.1088/0953-8984/18/46/013

Study on fatigue and breakdown properties of Pt/(Pb, Sr)TiO_3/Pt capacitors

Jyh-Liang Wang[1], Yi-Sheng Lai[2], Bi-Shiou Chiou[1], Huai-Yuan Tseng[1], Chun-Chien Tsai[1], Chuan-Ping Juan[1], Chueh-Kuei Jan[1] and Huang-Chung Cheng[1]

[1] Department of Electronics Engineering and Institute of Electronics, National Chiao Tung University, 1001 Ta Hsueh Road, Hsinchu 30010, Taiwan
[2] Department of Materials Science and Engineering, National United University, Miaoli 36003, Taiwan

E-mail: freeair.ee88g@nctu.edu.tw

Received 5 September 2006, in final form 11 October 2006
Published 3 November 2006
Online at stacks.iop.org/JPhysCM/18/10457

Abstract

Pulsed-laser deposited (Pb, Sr)TiO_3 (PSrT) films on Pt/SiO_2/Si substrate at various ambient oxygen pressures (P_{O_2}) are investigated in this work. Films deposited at P_{O_2} below 100 mTorr exhibit the (100) preferred orientation and a tetragonal structure with larger tetragonality. In addition, films deposited at 80 mTorr exhibit the most apparent ferroelectric properties in contrast to those deposited at 200 mTorr. Moreover, films deposited at higher P_{O_2} also exhibit longer lifetimes and higher breakdown fields due to their smaller leakage current density, in terms of the reduction of defects, compensation of oxygen vacancies (OVs), an improved interface and small cluster sizes. An energy band model reveals that fatigue properties of PSrT films are dominated by interfacial states at low P_{O_2} and by deep trapping states at high P_{O_2}, which could be ascribed to OVs located at the interfaces and inside films, respectively.

1. Introduction

(Pb, Sr)TiO_3 (PSrT) is feasible for memory, sensor, frequency tuning devices and microwave applications due to its large electric-field-dependent dielectric constant and composition-dependent Curie temperature [1–6]. The PSrT film is constituted by a solid solution of $PbTiO_3$ (PTO) and $SrTiO_3$ (STO). PTO and STO films, at room temperature, behave as a tetragonal structure (ferroelectric phase) and a cubic structure (paraelectric phase), respectively, because PTO has the Curie temperature (T_c) at 490 °C and STO has the T_c at −220 °C. The effects of lead (Pb) substituted by strontium (Sr) in the PTO film decrease crystallization temperature and offer a good control of the dielectric properties at room temperature [1, 2].

 © 2006 IOP Publishing Ltd Printed in the UK

In this work, PSrT films were prepared using the pulsed-laser deposition (PLD) because of its simplicity, versatility, and capability of growing a wide variety of stoichiometric oxide films without subsequent high-temperature annealing. Thus, PLD is a potential technique which could be excellent for fabricating ceramic films with complex compounds and integrated into low-temperature semiconductor processing to protect the formerly fabricated structure from damage and eliminate the volatilization of PbO in lead titanate-based thin films, which always degrades the crystallinity of perovskite phases and the electric properties of ferroelectric devices [7]. The pulsed-laser deposition process consists of three steps [8]: (1) vaporization of a target material by laser beam, (2) transport and interaction of a vapour plume with a background ambient, and (3) condensation of the ablated material onto a substrate where a thin film nucleates and grows. Hence, the structural and the electrical characteristics of PLD ferroelectric films are strongly affected by the processing parameters, such as substrate temperature, laser energy fluence (laser power density) and oxygen ambience.

Lots of studies on ferroelectric films have focused on the platinum electrode system which gives good stability to lead-based perovskite materials [9]. The noble metal platinum (Pt) is considered as the electrode of the Pt/PSrT/Pt capacitor also because of its low power consumption and low RC delay [6], compared to the conductive oxides [9], such as (La, Sr)CoO_3, (La, Sr)MnO_3, or RuO_2. Nevertheless, the polarization degradation of lead-based ferroelectric films has been constantly observed for a metal electrode when Pt is employed [7, 9, 10]. Some studies about the effect of ambient oxygen pressure (P_{O_2}) on PLD ferroelectric films have been reported [11–14]. However, the effect of P_{O_2} on PLD PSrT films prepared on Pt/SiO_2 substrate and their according reliability properties have not been addressed much. Therefore, the purpose of this study is focused on the properties of polarization switching degradation (fatigue) and breakdown of PSrT films deposited with various ambient oxygen pressures by the low-temperature PLD technique.

2. Experimental procedures

The 100 nm thick platinum (Pt) film was sputtered onto SiO_2/p-type Si as the bottom electrode followed by annealing at 450 °C for 30 min in N_2 ambient. Thin PSrT films with 200 nm in thickness were deposited on Pt/SiO_2/Si substrate electrodes with a KrF pulsed-laser deposition system (Lambda Physik Excimer Laser LPX 200i, $\lambda = 248$ nm). A set of optical lenses was used to focus the excimer laser beam onto the $(Pb_{0.6}, Sr_{0.4})TiO_3$ target in vacuum. The PSrT target was prepared with a conventional ceramic fabrication process [8]. The vacuum chamber was pumped down to a base pressure of 0.1 mTorr and then refilled with O_2 as reactive gas. The vaporized species of the target transferred and deposited on the substrate heated by a thermal heater. The target to substrate distance was 4 cm. The deposition temperature was fixed at a low substrate temperature of 400 °C, calibrated at the wafer upper surface. The ambient oxygen pressure (P_{O_2}) was varied from 50 to 200 mTorr. During the PLD process, the laser pulse rate and the average energy fluence were 5 Hz and 1.55 J cm^{-2} per pulse, respectively.

The film thickness and the surface morphology of PSrT films were examined by field emission scanning electron microscopy (FESEM) (S-4000, Hitachi). An Auger electron spectroscope (AES) (Auger 670 PHI Xi, Physical Electronics) was used to analyse the element ratios on the surface of PSrT films. The crystallinity of the film was analysed by x-ray diffractometer (D5000, Siemens, using Cu Kα, $\lambda \sim 0.154$ nm).

After the physical examinations, the Pt top electrodes, with a thickness of 100 nm and a diameter of 75 μm, were deposited by sputtering and patterned by a shadow mask process to form a Pt/PSrT/Pt capacitor structure. An automatic measurement system that combines an IBM PC/AT, a semiconductor parameter analyser (4156C, Agilent Technologies) and a

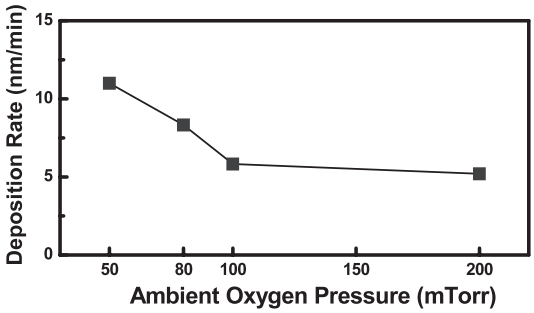

Figure 1. Deposition rate of PLD PSrT films prepared at various ambient oxygen pressures (P_{O_2}) on Pt/SiO_2/Si.

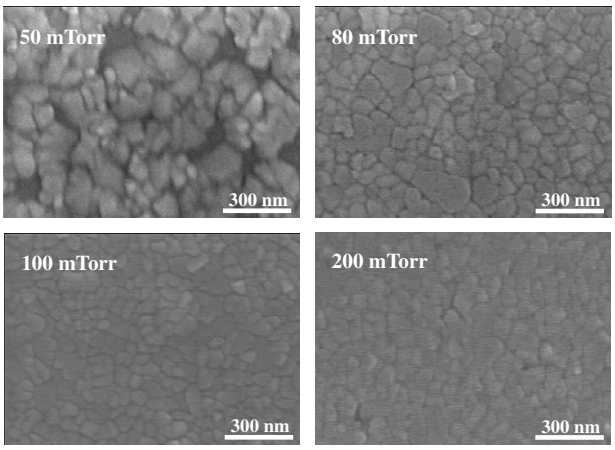

Figure 2. SEM surface morphologies of PLD PSrT films deposited at various ambient oxygen pressures on Pt/SiO_2/Si.

probe station was used to measure the leakage current (I–V characteristics) and breakdown properties. The ferroelectric polarization versus electric field (P–E) characteristics of the PSrT film were determined directly by virtual ground circuits (RT-66A standardized ferroelectric testing system, Radiant Technologies). A pulse generator (8110A, Hewlett Packard) and a pulse/function generator (8116A, Hewlett Packard) were connected together with low noise BNC cables to generate a $+3$ V/-3 V bipolar wave pulsed at 1 MHz, confirmed by an oscilloscope (54645A, Hewlett Packard), as an input signal for the measurement of polarization switching degradation (fatigue).

3. Results and discussion

PLD PSrT films were prepared at various ambient oxygen pressures (P_{O_2}). Figure 1 shows that the deposition rate of PSrT films is maximum at $P_{O_2} = 50$ mTorr and then decreases as P_{O_2} increases due to the increasing collisions between ejected species and the ambient oxygen gas. Moreover, film thickness could be controlled and roughly considered as a time-based function for different P_{O_2}. In general, the situation of collisions affects the stacking of clusters during PLD, which directly associates with morphologies and structural characteristics of films [8]. Figure 2 shows SEM surface morphologies of PLD PSrT films deposited at various P_{O_2} on

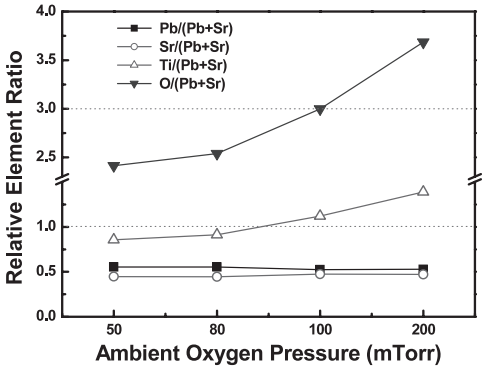

Figure 3. Relative element ratios of PSrT films deposited at various ambient oxygen pressures on $Pt/SiO_2/Si$.

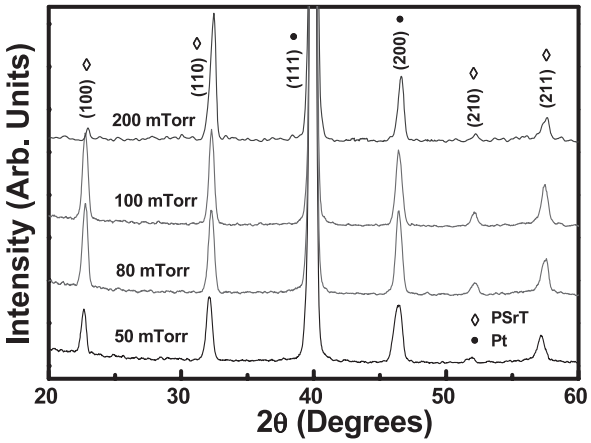

Figure 4. X-ray diffraction spectra of PSrT films deposited at various ambient oxygen pressures on $Pt/SiO_2/Si$.

$Pt/SiO_2/Si$ (100) wafers. As the P_{O_2} increases, the morphology becomes denser and less porous, and the clusters gradually become more uniform, rounded and small, which reflects the better stacking of clusters and fewer defects. Usually, the grain size may be confined by the size of a cluster. Thus, a larger cluster may connect to larger grain size and fewer grain boundaries. We will address later, as a result of the electrical characteristics, that the dense morphology of PSrT films deposited at higher P_{O_2} exhibits fewer interfacial states and fewer deep trapping states inside films. Figure 3 presents the element ratios, calibrated with the stoichiometric composition of the $(Pb_{0.6}, Sr_{0.4})TiO_3$ target, on the surface of PSrT films analysed by the AES technique, and reveals that the film composition is a function of P_{O_2}. It can be seen that the element ratio of $Ti/(Pb + Sr)$ increases markedly with the increase of P_{O_2} as opposed to the element ratio of $Pb/(Pb + Sr)$. Besides, the element ratio of $Sr/(Pb + Sr)$ slightly varies with P_{O_2}. It also indicates that the element ratio of $O/(Pb + Sr)$ increases from 2.41 to 3.69 as P_{O_2} increases. This suggests that the oxygen content of films can be strongly compensated at higher P_{O_2}.

Figure 4 displays the x-ray diffraction (XRD) spectra of PSrT films deposited at various P_{O_2} on $Pt/SiO_2/Si$ (100) wafers. All the diffraction peaks of these spectra are indexed as

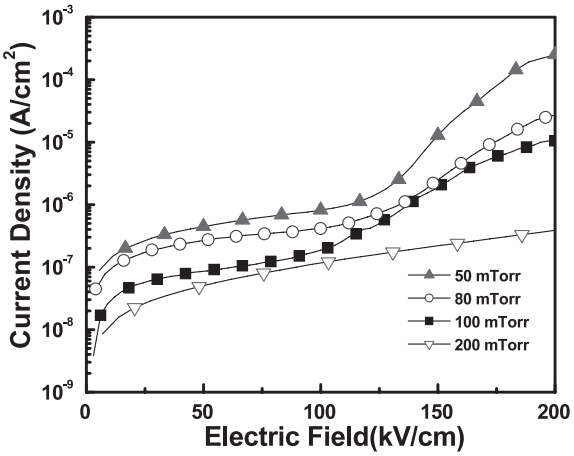

Figure 5. Current density versus electric field (J–E) characteristics of Pt/PSrT/Pt capacitors applied at positive bias.

(100), (110), (210) and (211) planes of $(Pb_{1-x}Sr_x)TiO_3$ perovskite phases [1, 2, 6, 15–18]. The crystalline PSrT films are observed at such low temperature (400 °C) because (1) the addition of strontium induces a lower crystallization temperature of PSrT than that of PZT [1] and (2) the PLD technique can preserve the crystalline phase and stoichiometric ratio of the target material at low substrate temperature [8]. Moreover, the intensity of the (100) and (110) diffraction peaks varies significantly as P_{O_2} increases. In figure 4, the relative intensity of the (110) orientation increases with increasing P_{O_2} and shows a maximum at $P_{O_2} = 200$ mTorr. In contrast, the relative intensity of the (100) orientation exhibits a little variation when $P_{O_2} \leqslant 100$ mTorr and then decreases noticeably as P_{O_2} increases from 100 to 200 mTorr. A transition from (100) preferred orientation to (110) preferred orientation of PSrT films is observed as P_{O_2} increases above 100 mTorr. Furthermore, the PSrT films have a tetragonal structure with a clear (100) diffraction peak for $x < 0.5$ and a cubic structure with a strong (110) diffraction peak for $x \geqslant 0.5$, as reported in previous works [1, 2]. On the other hand, the tetragonalities (c/a), i.e. the ratios of c-axis/a-axis lattice constant obtained by electron diffraction patterns (not shown in this work), of the PSrT films deposited at 50 and 200 mTorr are ∼1.033 and ∼1, respectively. The larger tetragonality for films deposited at lower P_{O_2} may be attributed to the oxygen deficiency [19–21]. This suggests that the structure of PSrT films deposited with P_{O_2} below 100 mTorr is tetragonal, consistent with the low element ratio of O/(Pb + Sr) (figure 3). In short, it is clear that the surface morphology, stoichiometric composition, preferred orientation, and tetragonality of PSrT films could apparently be affected by ambient oxygen pressures during PLD.

Figure 5 displays the current density versus electric field (J–E) characteristics of Pt/PSrT/Pt capacitors under positive bias. It is found that the leakage current is reduced when P_{O_2} increases. The inhibited leakage current observed in PSrT films deposited at higher P_{O_2} will be correlated with the more compensated oxygen vacancies (OVs) due to the larger oxygen element ratio as shown in figure 3. The OVs will act as charged defects to degrade leakage currents as expressed by the following reaction [22–24]:

$$O_o \leftrightarrow V_o^{\bullet\bullet} + 2e' + \tfrac{1}{2}O_2, \tag{1}$$

where O_o, $V_o^{\bullet\bullet}$, and e' represent the oxygen ion on its normal site, the oxygen vacancy, and the electron, respectively. Figure 6 displays the characteristics of time-dependent dielectric

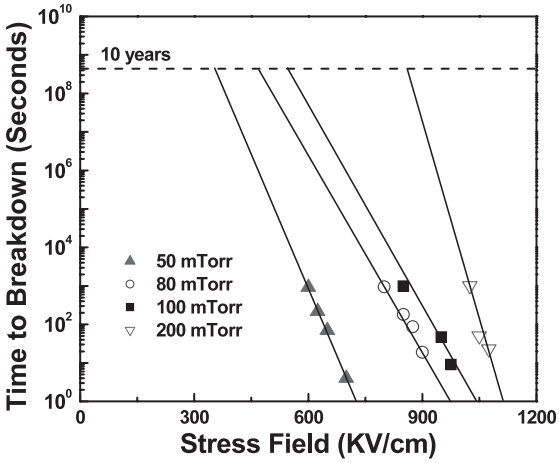

Figure 6. TDDB characteristics (time to breakdown as a function of electric field) for PSrT films deposited at various P_{O_2}.

breakdown (TDDB) to predict the 10 year lifetime. TDDB is regarded as the resistance degradation of dielectric films, which slowly increases the leakage current under constant temperature and dc field stress. The mechanism of resistance degradations in perovskite films could be categorized into the grain boundary model and the reduction model [22–24]. The grain boundary model indicates a large potential drop across the high-resistivity grain boundary. Films with smaller grain sizes exhibit more grain boundaries, resulting in the shared drop in voltage and the suppressed resistance degradation. On the other hand, the reduction model suggests that OVs and injection electrons cause resistance degradation. Consequently, PSrT films deposited at higher P_{O_2} exhibit longer lifetime and higher breakdown field due to their smaller leakage current density (figure 5), in terms of the reduction of defects, compensation of OVs (i.e. larger oxygen concentration shown in figure 3), an improved interface (i.e. the denser, less porous and more uniform morphology shown in figure 2), and small cluster sizes.

Figure 7 presents the saturation polarization ($2P_s$), remnant polarization ($2P_r$), and coercive field ($2E_c$) values of PSrT films vary with P_{O_2}. The maximum values of films deposited at 400 °C and 80 mTorr are 29.08 μC cm^{-2}, 6.65 μC cm^{-2}, and 90.0 kV cm^{-1}, respectively, which are comparable to those of PSrT films prepared by the sol-gel process at temperatures higher than 700 °C [1, 6]. In contrast, films deposited at 200 mTorr reveal extremely small and indistinct ferroelectricities. The polarization of the lead titanate-based crystal is maximum in the [100] direction, so the polarizations of the films enhanced with the preferred (110) orientation are weaker than those of the films with the preferred (100) orientation [9, 25]. As mentioned above, PSrT films deposited with P_{O_2} below 100 mTorr exhibit the (100) preferred orientation and a tetragonal structure with larger tetragonality. Because the ferroelectric dipole originates from ionic displacement in the *c*-axis direction, large spontaneous polarization is obtained with the elongated *c*-axis, i.e. the larger tetragonality. In other words, the ferroelectricity of PSrT films is the combined effect of the preferred orientation and oxygen content. Thus, the PSrT film deposited at 80 mTorr exhibits the most apparent ferroelectric properties, which are connected with the enhanced (100) preferred orientation (figure 4) and the larger oxygen concentration (figure 3). Table 1 summarizes the physical properties and electrical characteristics of PLD PSrT films deposited at various ambient oxygen pressures on Pt/SiO_2/Si (100) wafers.

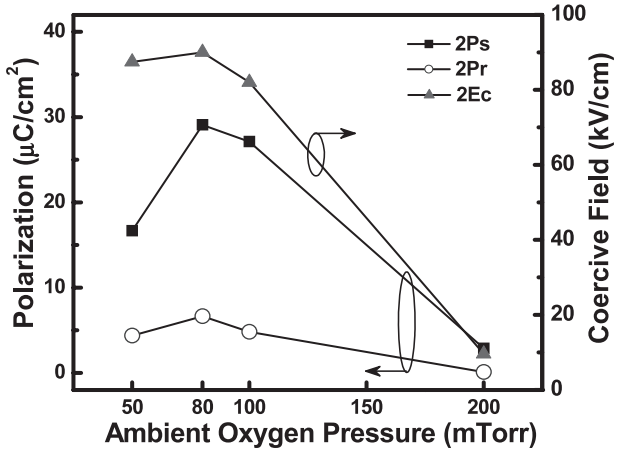

Figure 7. Saturation polarization ($2P_s$), remnant polarization ($2P_r$) and coercive field ($2E_c$) of Pt/PSrT/Pt capacitors prepared at various P_{O_2}.

Table 1. Summarized characteristics of PLD PSrT films deposited at various ambient oxygen pressures on Pt/SiO_2/Si (100) wafers.

Ambient oxygen pressure (P_{O_2}, mTorr)	50	80	100	200
Oxygen element ratio[a]	2.41	2.52	3.00	3.69
Leakage current density (μA cm^{-2})[b]	0.812	0.416	0.187	0.119
Time-zero breakdown field (kV cm^{-1})[c]	721	976	1042	1117
Saturation polariztion ($2P_s$, μC cm^{-2})[d]	16.67	29.08	27.13	2.87
Remanent polarization ($2P_r$, μC cm^{-2})[d]	4.36	6.65	4.82	0.09
Coercive field ($2E_c$, kV cm^{-1})[d]	87.5	90.0	82.0	9.6

[a] Evaluated from AES analysis.
[b] Evaluated from J–E curves biased at +100 kV cm^{-1}.
[c] Evaluated from TDDB curves.
[d] Evaluated from P–E hysteresis loops.

Figure 8 demonstrates the properties of remnant polarization (P_r) fatigue of Pt/PSrT/Pt capacitors after the switching operation. This fatigue examination does not include the film deposited at 200 mTorr because of its indistinct ferroelectricities. Films deposited at 80 mTorr start to fatigue from 10^8 switching cycles and reveal a slight degradation in P_r (<17%) after 10^{10} switching cycles. From previous works [26–29], it has been pointed out that the space charge of OVs can be the major fatigue contributor. The fatigue process will alter the space charge distribution and reduce the Schottky barrier height at the interface of electrodes, leading to the change of leakage currents. Later in the text, the leakage current data before/after fatigued switching operation are interpreted as Schottky emission (SE) at lower electric fields and Poole–Frenkel emission (PF) at higher electric fields to analyse the space charge correlated to interface-limited and bulk-limited characteristics, accordingly [24, 30, 31]. The SE and PF behaviour are expressed as

$$\text{SE:} \quad \log(J_{SE}/T^2) = -q[\varphi_B - (qE/4\pi\varepsilon_d\varepsilon_0)^{1/2}]/(kT\ln 10) + \log(A^*), \quad (2)$$

$$\text{PF:} \quad \log(J_{PF}/E) = -q[\varphi_t - (qE/\pi\varepsilon_d\varepsilon_0)^{1/2}]/(kT\ln 10) + \log(B), \quad (3)$$

where A^* is the effective Richardson's constant, B is a constant, φ_B is the potential barrier height at the interface, φ_t is the trapped energy level, ε_d is the dynamic dielectric constant of the

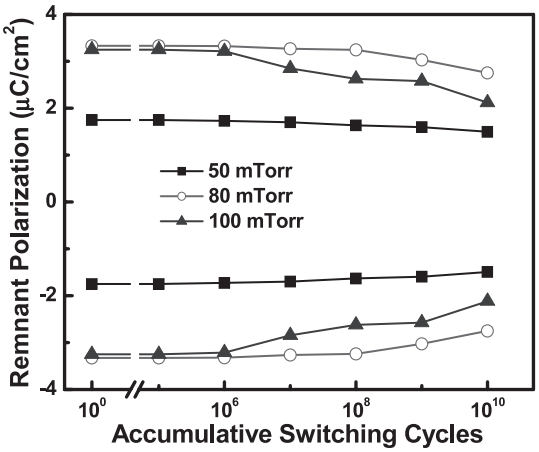

Figure 8. The fatigue behaviours of remnant polarization (P_r) versus accumulative switching cycles of Pt/PSrT/Pt capacitors prepared at various P_{O_2}.

ferroelectric material in the infrared region, q is the unit charge, k is Boltzmann's constant, T is absolute temperature, and E is the external electric field. If the conduction current follows SE behaviour, then a $\log(J/T^2)$ against $E^{1/2}$ plot should be linear. Similarly, a $\log(J/E)$ against $E^{1/2}$ plot can be made for PF. Figure 9(a) presents the SE plot of fresh and fatigued Pt/PSrT/Pt capacitors deposited at various P_{O_2} and the dashed lines are the fitted results. The inhibited leakage current biased at lower electric fields of PSrT films deposited at higher P_{O_2} is correlated with the lower Schottky barrier, fewer interfacial states, and fewer space charges (charged OVs) due to the improved interface (figure 2) and compensated OVs. This suggests that the films deposited at higher P_{O_2} have fewer interface states before being fatigued and exhibit nearly fatigue-free J–E characteristics at lower electric fields. Figure 9(b) shows the PF plot using the same experimental current–voltage (I–V) data. Likewise, the inhibited leakage current of films deposited at higher P_{O_2} and biased at higher electric fields is associated with less deep trapping states and fewer space charges (charged OVs) inside films due to compensated OVs. It indicates that the onset of PF behaviours of fresh Pt/PSrT/Pt capacitors appears when the bias exceeds $+130$ kV cm^{-1}. In contrast, the onset of PF behaviours of fatigued Pt/PSrT/Pt capacitors changes from above $+130$ to $+90$ kV cm^{-1} when P_{O_2} increases from 50 to 100 mTorr. This suggests that films deposited at higher P_{O_2} exhibit fewer interfacial states with an improved interface, which inhibit OVs generating and accumulating at the interface of electrodes, but prefer to create OVs inside films after fatigue.

Figure 10 illustrates the electron energy band of PSrT films and shows that the interfaces of substrate electrodes act as n-type semiconductors due to the generation of oxygen vacancies in ABO_3 perovskites [24, 26]. It reveals that PSrT films deposited at lower P_{O_2} have porous surface and more OVs than those deposited at higher P_{O_2}, yielding more interfacial states and more trapping states inside films. As a result, there are more OVs accumulated at the interface and the fatigue properties are dominated by the interfacial states. Conversely, PSrT films deposited at higher P_{O_2} exhibit improved interfaces and compensated OVs, yielding fewer interfacial states and fewer deep trapping states inside films. It suggests that OVs are generated inside films and the fatigue properties are dominated by deep trapping states. Hence, films deposited at 80 mTorr exhibit nearly fatigue-free J–E characteristics at lower electric fields and a higher onset field of PF behaviours of fatigued Pt/PSrT/Pt capacitors. The results could be connected with the compensated OVs and a balance distribution of OVs located at the interfaces

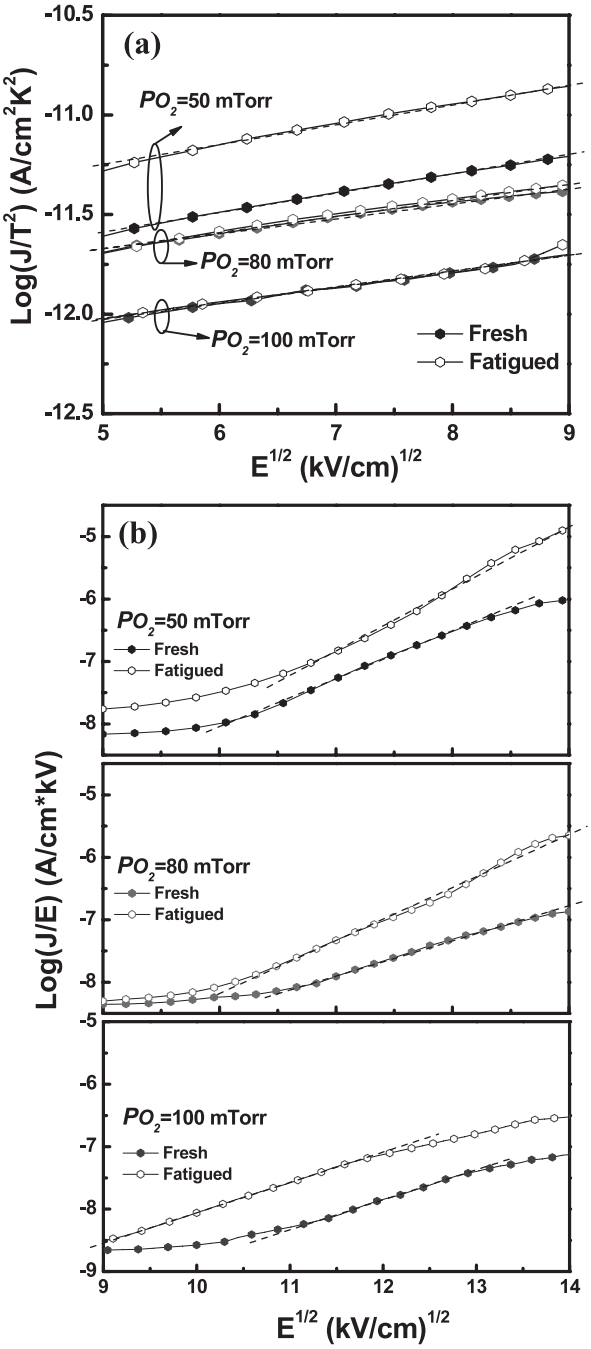

Figure 9. (a) Schottky emission plot fitting of $\log(J/T^2)$ versus $E^{1/2}$ and (b) Poole–Frenkel emission plot fitting of $\log(J/E)$ versus $E^{1/2}$ for the fresh and fatigued Pt/PSrT/Pt capacitors prepared at various P_{O_2}.

and inside films, corresponding to the optimum fatigue resistance with fatigue starting from 10^8 switching cycles.

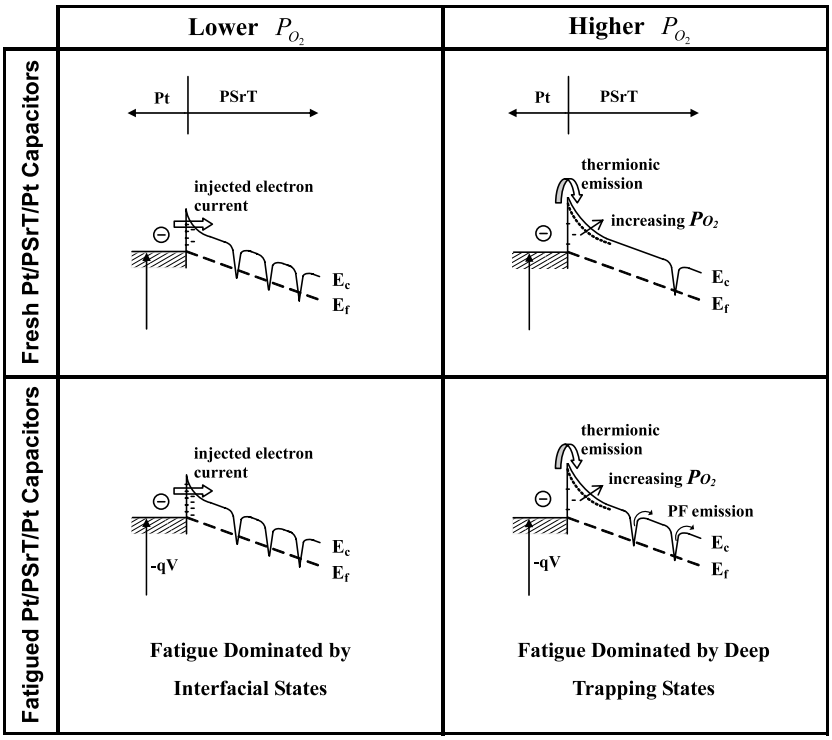

Figure 10. Schematic drawings of the electron energy band for the fresh and fatigued Pt/PSrT/Pt capacitors deposited at low and high P_{O_2}.

4. Conclusions

The surface morphology, film composition, crystallographic orientation and electrical characteristics of PSrT films are found to be influenced by ambient oxygen pressures during low-temperature PLD. PSrT films deposited with P_{O_2} below 100 mTorr exhibit the (100) preferred orientation and a tetragonal structure with larger tetragonality. Thus, films deposited at 80 mTorr have the most apparent ferroelectric properties. In contrast, films deposited at 200 mTorr reveal extremely small and indistinct ferroelectricities. Films deposited at higher P_{O_2} also exhibit longer lifetime and higher breakdown field due to their smaller leakage current density, in terms of the reduction of defects, compensation of OVs, an improved interface and small cluster sizes. It also suggests that PSrT films deposited at lower P_{O_2} have porous surface and more OVs than those deposited at higher P_{O_2}, yielding more interfacial states and more trapping states inside films, and the fatigue properties are dominated by the interfacial states. Conversely, PSrT films deposited at higher P_{O_2} show improved interfaces and compensated OVs, yielding fewer interfacial states and fewer deep trapping states inside films, and the fatigue properties are dominated by deep trapping states.

Acknowledgments

This work was supported in part by the National Science Council of ROC under the contract NSC94-2218-E-009-028. Thanks are also due to the Nano Facility Center (NFC) in National

Chiao Tung University and the National Nano Device Laboratory (NDL) of the NSC for technical support.

References

[1] Kang D H, Kim J H, Park J H and Yoon K H 2001 *Mater. Res. Bull.* **36** 265
[2] Zhang F, Karaki T and Adachi M 2005 *Japan. J. Appl. Phys.* **44** 6995
[3] Karaki T, Du J, Fujii T and Adachi M 2002 *Japan. J. Appl. Phys.* **41** 6761
[4] Chou C C, Hou C S, Chang G C and Cheng H F 1999 *Appl. Surf. Sci.* **142** 413
[5] Chou C C, Hou C S and Cheng H F 1998 *Ferroelectrics* **206/207** 393
[6] Hou C S, Pan H C, Chou C C and Cheng H F 1999 *Ferroelectrics* **232** 129
[7] Lim D G, Park Y, Moon S I and Yi J 2000 Applications of ferroelectrics 2000 *ISAF 2000: Proc. 2000 12th IEEE Int. Symp. (Honolulu)* (Piscataway, NJ: IEEE) p 599
[8] Chrisey D B and Huber G K 1992 *Pulsed Laser Deposition of Thin Films* (New York: Wiley–Interscience) pp 55–87, 167–98
[9] De Araujo C P, Scott J F and Taylor G W 1996 *Ferroelectric Thin Films: Synthesis and Basic Properties, Ferroelectric and Related Phenomena* vol 10 (Netherlands: Gordon and Breach) pp 193–226, 447–78
[10] Wang Y, Wang K F, Zhu C and Liu J M 2006 *J. Appl. Phys.* **99** 044109
[11] James A R and Prakash C 2004 *Appl. Phys. Lett.* **84** 1165
[12] Scarisoreanu N, Craciun F, Dinescu G, Verardi P and Dinescu M 2004 *Thin Solid Films* **453/454** 399
[13] Rodrigueza R C, Sanchezb S P, Wattsb B E and Leccabue F 2003 *Mater. Lett.* **57** 3958
[14] Gao X S, Xue J M, Li J, Ong C K and Wang J 2003 *Microelectron. Eng.* **66** 926
[15] Chou C C, Chang H Y, Lin I N, Shaw B J and Tan J T 1998 *Japan. J. Appl. Phys.* **37** 5269
[16] Pan H C, Chang G C, Chou C C and Cheng H F 1999 *Integr. Ferroelectr.* **25** 179
[17] Chung H J, Kim J H and Woo S I 2001 *Chem. Mater.* **13** 1441
[18] Chung H J and Woo S I 2001 *J. Vac. Sci. Technol.* B **19** 275
[19] Li C L, Chen Z H, Zhou Y L and Cui1 D F 2001 *J. Phys.: Condens. Matter* **13** 5261
[20] Fuchs D, Adam M, Schweiss P, Gerhold S, Schuppler S, Schneider R and Obst B 2000 *J. Appl. Phys.* **88** 1844
[21] Cui D F, Wang H S, Chen Z H, Zhou Y L, Lu H B and Yang G Z 1997 *J. Vac. Sci. Technol.* A **15** 275
[22] Waster R, Baiatu R T and Haratl K H 1990 *J. Am. Ceram. Soc.* **73** 1645
[23] Tsai M S and Tseng T Y 2000 *IEEE Trans. Compon. Packag. Technol.* **23** 128
[24] Shye D C, Chiou B S, Lai M J, Hwang C C, Jiang C C, Chen J S, Cheng M H and Cheng H C 2003 *J. Electrochem. Soc.* **150** F20
[25] Xu Y 1991 *Ferroelectric Materials and Their Applications* (Amsterdam: Elsevier Science Publishers B. V.) pp 101–62
[26] Scott J F 2000 *Ferroelectric Memories* (Berlin: Springer) pp 79–85, 134–43
[27] Jiang A Q, Scott J F, Dawber M and Wang C 2002 *J. Appl. Phys.* **92** 6756
[28] Dawber M and Scott J F 2000 *Appl. Phys. Lett.* **76** 1060
[29] Bratkovsky A M and Levanyuk A P 2001 *Phys. Rev.* B **63** 132103
[30] Vorobiev A, Rundqvist P, Khamchahe K and Gevorgian S 2004 *J. Appl. Phys.* **96** 4642
[31] Ezhivalavan S, Samper V, Seng T W, Junmin X and Wang J 2004 *J. Appl. Phys.* **96** 2181